Photodetachment Spectra of Trapped Electrons in Spherical Potentials

T. Kajiwara, K. Funabashi, and C. Naleway
Department of Chemistry and the Radiation Laboratory, *
University of Notre Dame, Notre Dame, Indiana 46556
(Received 6 March 1972)

The line shapes of absorption spectra of trapped electrons in metal-ammonia solutions, water, and alcohols are compared in detail with photodetachment spectra of spherical potentials, which have been applied extensively in liquid helium. A qualitative discussion is presented to point out some uncertainty in the role of the bound-bound transition $1s \rightarrow 2p$, which is predominant in the dielectric continuum model. Apart from the uncertainty related to the effective mass of the polaron, the coherence of the $2p$ state in the more realistic fluctuation potential is likely to be small. A molecular model for the trapped electrons is briefly described.

I. INTRODUCTION

In this paper, we propose a phenomenological model for the absorption spectra of solvated electrons in noncrystalline polar media. The essential feature of the model is the use of a finite-range potential with only one bound state, in contrast to the more familiar polaron potential with a screened Coulomb potential.[1] Although the polaron model predicts the transition energies corresponding to absorption maxima with reasonable choice of parameters, the broadness and asymmetry of the spectral profile could not be generated without introducing additional parameters such as a distribution of cavity size. Judging from the stability of the line shape with respect to the decay time and also to the temperature in systems such as metal-ammonia solutions and liquid water, it is difficult to believe that a distribution of the trap depths or vibronic couplings, which undoubtedly contribute to the spectral profiles to some extent, is the major factor for the observed spectral profiles.

The spherical potential well, which is the simplest model for finite-range potentials, has been applied for photodisintegration of deuteron[2] and for the trapped electrons in liquid helium.[3-6] The photodetachment spectra of spherical potentials, however, have not been compared in detail with the absorption spectra of the trapped electrons in molecular liquids. Although the basic elements of the spherical potential are well known[7] and quite straightforward, the actual computation is rather complicated because of the interference effect of the virtual states (p-wave resonance in particular) with the plane-wave states. The line shapes of the photodetachment spectra turn out to be sensitive functions of the parameters: the range and the depth of the potential. The spherical potentials studied by Breit and Condon[2] and by Wang[6] were found to be either too shallow or too deep for met-al-ammonia solutions, water, and alcohols.

Clearly, the spherical potential is a drastic simplification of very complicated real potentials. But the choice of other forms of potentials, such as a rounded potential proposed by Springett,[8] does not seem to have a definite advantage over the spherical potential, at least in our problem, because of the unknown factor associated with the use of less accurate wave functions and also with the physical meanings of additional parameters.

As long as a finite-range potential contains only one bound state, the optical response of the trapped electron in the potential is always a broad band regardless of the detailed difference in the form of the potential. As discussed in Sec. IV of this paper, the range and the depth of the potential arise from fluctuation in transfer and polarization energies within the framework of tight-binding approximation. In polar systems, with which we are concerned, there is additional potential which arises from relaxation of permanent dipole moments. The latter is approximated by a smooth Coulomb potential in the dielectric continuum model.[9] In this model, the $2p$ state in the long-range Coulomb potential is the most important state in determining the absorption maximum.[1] It has been pointed out by Fröhlich[9] that the Coulomb potential alone does not necessarily localize an electron and also the actual potential is more flat than a Coulomb potential when the excess charge is regarded as a particle rather than a source of a field. The role of the Coulomb potential depends upon the effective mass of the polaron, which is beyond the scope of this article. In Sec. II, we examine the physical significance of the smooth Coulomb potential in terms of more realistic fluctuation potentials and indicate that the coherence of the $2p$ state is too small to be meaningful for further elaboration, such as a detailed consideration of the vibronic linewidth of the $2p$ state.

II. ROLE OF BOUND STATES IN ABSORPTION SPECTRA

Let us begin with the description of a localized electron in the conventional dielectric continuum model. The electron feels a Coulomb potential at large distances from the center of localization because of the difference in the optical and static dielectric constants. Because of the finite extension of the electron distribution, the short-range interaction is of a non-Coulombic type which can be quite complicated, but could be approximated, for example, by a square well potential for computational purposes. This type of potential in general accommodates a large number of excited states in addition to the ground state because of the long-range character of the Coulomb potential. In this case, the optical response of the ground-state electron can be described as a sum of all transitions to the excited states and the ionized states. Unless one introduces additional parameters besides the shape of the short-range potential, the largest oscillator strength is taken up by the transition corresponding to $1s \to 2p$. The peak of the absorption spectrum is likely to correspond to the transition energy $1s \to 2p$, while the line shape or the broadness might be "explained" by vibronic interactions or by a distribution of the trap depths arising from fluctuation of the short-range potentials near the center of the localization.

It is therefore crucial to understand the role and the meaning of the $2p$ state in the context of the dielectric continuum model. For this purpose, let us consider the physical meaning of the long-range Coulombic potential which is "smooth" in the dielectric continuum model. If one examines the electron potential on a microscopic or molecular-scale level, one finds that the potential is by no means a smooth one, but is fluctuating from site to site. This fluctuating potential arises from a short-range and instantaneous interaction of the electron with its immediate vicinity. To convince ourselves on this point, consider the potential at a given distance R from the center of localization. The potential depends upon the nature of the point under consideration: whether it is right on top of a molecule, or whether it is an intermolecular site of varying surroundings. The order of magnitude of such a fluctuation potential is estimated to be 1 eV. This situation is schematically drawn in Fig. 1. The smooth potential of the dielectric continuum model is then considered to be an ensemble average of these fluctuating potentials whose patterns are different for different electrons. Let the smooth potential be V_s and the fluctuating potential belonging to the αth electron be V_α; then we have

$$V_s = \langle V_\alpha \rangle , \qquad (2.1)$$

where $\langle \ \rangle$ means the ensemble average. The po-

tential V_s has a set of eigenfunctions, ϕ^s_{1s}, ϕ^s_{2p},...., which satisfy the Schrödinger equations

$$H_s \, \phi^s_i = \epsilon^s_i \, \phi^s_i , \qquad i = 0, 1, 2, \ldots \qquad (2.2)$$

where

$$H_s = -\tfrac{1}{2} \Delta + V_s , \qquad (2.3)$$

where $-\tfrac{1}{2}\Delta$ is the kinetic-energy operator in atomic units. The transition probability corresponding to the transition energy, $\hbar\omega$, is given by

$$|M^s(\omega)|^2 = \sum_i |(\phi^s_0 | e\vec{r} | \phi^s_i)|^2 \, \delta(\hbar\omega - \epsilon^s_i + \epsilon^s_0) , \qquad (2.4)$$

where $\phi^s_0 = \phi^s_{1s}$.

The eigenfunctions belonging to the Hamiltonian H_α,

$$H_\alpha = -\tfrac{1}{2}\Delta + V_\alpha , \qquad (2.5)$$

are not simple, but are calculable in principle. They satisfy

$$H_\alpha \phi^\alpha_j = \epsilon^\alpha_j \, \phi^\alpha_j , \qquad j = 0, 1, 2, \ldots \qquad (2.6)$$

where the subscript j designates the eigenstates in which the angular momentum may not be a good quantum number. The transition probability for the αth electron can be written as

$$|M^\alpha(\omega)|^2 = \sum_j |(\phi^\alpha_0 | e\vec{r} | \phi^\alpha_j)|^2 \, \delta(\hbar\omega - \epsilon^\alpha_j + \epsilon^\alpha_0) . \qquad (2.7)$$

An experimentally observed spectrum corresponds to the ensemble average of (2.7) over a large number of α.

The basic premise of the dielectric continuum model is to assert that

$$|M^s(\omega)|^2 \approx \langle |M^\alpha(\omega)|^2 \rangle . \qquad (2.8)$$

In order to understand the range and the condition of validity of (2.8), let us introduce the following assumptions. The short-range potential near the center of localization in each structure α has the same form and is so strong that the ground-state wave functions ϕ^α_0 and their binding energies ϵ^α_0 are all equal to ϕ^s_0 and ϵ^s_0, respectively. With these assumptions, (2.7) can be written as

$$|M^\alpha(\omega)|^2 = \sum_j |(\phi^s_0 | e\vec{r} | \phi^\alpha_j)|^2 \, \delta(\hbar\omega - \epsilon^\alpha_j + \epsilon^s_0) . \qquad (2.9)$$
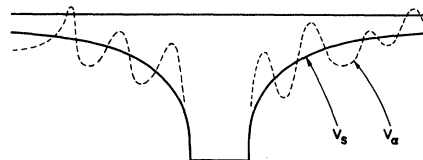

FIG. 1. Schematic electron potentials in polar media. The smooth solid line is that of the dielectric continuum model and the dotted line includes the effect of fluctuation potentials of disordered molecular arrangement. The central part is drawn as that of a square well, but the argument in the text is independent of the detailed nature of the short-range potential.

The ensemble averaging in (2.8) is reduced to the problem of finding the average of ϕ_j^α, which can be expanded in terms of ϕ_i^s as

$$\phi_j^\alpha = \phi_i^s + \sum_k \frac{\phi_k^s(\phi_k^s|\Delta V_\alpha|\phi_j^\alpha)}{\epsilon_j^\alpha - \epsilon_k^s} \quad , \qquad (2.10)$$

where

$$\Delta V_\alpha = V_\alpha - V_s \qquad (2.11)$$

and

$$\epsilon_j^\alpha = \epsilon_i^s \; . \qquad (2.12)$$

Equation (2.12) can be satisfied for all ϵ_i^s because there are a large number of electrons in the system. Using (2.10) and (2.12), we get

$$\langle \phi_j^\alpha \rangle = \phi_i^s + \sum_k \frac{\phi_k^s(\phi_k^s|\langle \Delta V_\alpha \phi_j^\alpha \rangle)}{\epsilon_i^s - \epsilon_k^s} \; . \qquad (2.13)$$

It can be seen easily that if

$$\langle \Delta V_\alpha \phi_j^\alpha \rangle = \langle \Delta V_\alpha \rangle \langle \phi_j^\alpha \rangle \; , \qquad (2.14)$$

Eq. (2.8) is valid because

$$\langle \Delta V_\alpha \rangle = \langle V_\alpha \rangle - V_s = 0$$

by (2.1) and (2.11).

The validity of the dielectric continuum model, therefore, depends critically upon the statistical dependence or correlation between ΔV_α and the wave function ϕ_j^α. The quantitative estimate of the degree of this correlation is very complicated, but is closely related to the problem of finding the mean free path or the cross section for scattering as a function of the wave number of the electron in disordered systems. If the effective wave number k of the state ϕ_j^α, which is related to its binding energy by $\epsilon_j^\alpha = \hbar^2 k^2/2m$ from the virial theorem, is so small that $ka \ll 1$ (a is the lattice constant or the intermolecular separation), the wave function is insensitive to a small variation of the scattering potential ΔV_α. This is equivalent to the notion that an electron with a very long de Broglie wavelength cannot respond to a small fluctuation. This is known as the optical approximation. For the states corresponding to high Rydberg series, (2.14) is approximately valid.

On the other hand, when $ka \approx 1$, the wave function ϕ_j^α can respond easily to a variation in the potential ΔV_α. These two quantities are statistically dependent and (2.14) is not valid. In the scattering picture, this is the region of k in which the mean free path drops rather sharply to a length comparable to the intermolecular separation. For $ka \gg 1$, the mean free path increases again, but such a case is of no interest in our problem.

The binding energy of a $2p$ electron for $ka \approx 1$ would be about 1 eV for $a = 3.5$ Å. In this case, the $2p$ state is heavily mixed with other states which carry little transition moment from the ground state. The effective transition moment of $1s \rightarrow 2p$

is accordingly depleted. If the binding energy of $2p$ electron is 1 eV and the mean free path is 3.5 Å, the mean lifetime of the $2p$ state becomes of the order of 10^{-16} sec, which is less than the time required for the optical transition. Such a transition is not observable.

The physical significance of the long-range smooth potential is then limited only to high Rydberg states in a narrow region of energy just below the polaron conduction band, even if the long-range potential is at all relevant. In this paper, we ignore the contribution of these states to the absorption spectrum and concentrate on the bound-free transitions.

III. PHOTOIONIZATION CROSS SECTION

The purpose of this section is to outline the method of calculation for the photoionization cross section of an electron in a spherical potential well.[7] The depth of the potential V_0 and the binding energy of the lowest bound S state, E_0, will be expressed as

$$V_0 = \lambda V_c \qquad (\lambda > 1) \; , \qquad (3.1)$$

$$E_0 = \gamma V_c \qquad (\lambda > \gamma > 0) \; , \qquad (3.2)$$

where

$$V_c = \pi^2 \hbar^2 / 8ma^2 \qquad (3.3)$$

and a is the radius of the potential.

The wave function for the lowest bound S state is written as

$$\psi_0(r\theta\varphi) = R(r) Y_{00}(\theta\varphi) \; , \qquad (3.4)$$

where

$$Y_{00}(\theta\varphi) = 1/(4\pi)^{1/2} \; , \qquad (3.5)$$

$$R(r) = A_0 \frac{\sin[\frac{1}{2}\pi(\lambda - \gamma)^{1/2}(r/a)]}{r} \qquad (r < a) \qquad (3.6)$$

$$= C_0 \frac{\exp[-\frac{1}{2}\pi\gamma^{1/2} \cdot (r/a)]}{r} \qquad (r > a) \; . \qquad (3.7)$$

The coefficients A_0 and C_0 and the parameter γ can be determined by requiring the continuity of the logarithmic derivatives at $r = a$ and the normalization.

The continuum wave function, which is characterized by wave vector k, is written as[10]

$$\psi_k(r\theta\varphi) = V^{-1/2} \sum_{l=0}^{\infty} \sum_{m=-l}^{l} R_{lm}^k(r) Y_{lm}(\theta\varphi) \; , \qquad (3.8)$$

where

$$R_{lm}^k(r) = B_{lm} j_l(\alpha_c r) \quad (r < a) \qquad (3.9)$$

$$= A_{lm}[(\cos\delta_l) j_l(kr) - (\sin\delta_l) n_l(kr)]$$
$$(r > a) \; , \qquad (3.10)$$

$$\alpha_c \equiv (\pi/2a)(\lambda + \kappa)^{1/2} \; , \qquad (3.11)$$

$$\kappa V_c \equiv \hbar^2 k^2 / 2m \; , \qquad (3.12)$$

$$A_{lm} = 4\pi(2l+1) i^l e^{-i\delta_l} Y^*(\theta_\kappa \varphi_\kappa) \; , \qquad (3.13)$$

$$B_{lm} = A_{lm} \frac{(\cos\delta_l) j_l(ka) - (\sin\delta_l) n_l(ka)}{j_l(\alpha_c a)} .$$

$$(3.14)$$

In (3.8)–(3.14), j_l and n_l are the spherical Bessel and Neumann function, respectively, δ_1 is the phase shift, θ_κ and φ_κ express the direction of the ejected electron, and V is the volume of the system which is to be made very large eventually.

The differential cross section of photoionization into the solid angle $d\Omega$ is given when the polar axis (or the z axis) is taken to be parallel to the direction of electric vector of incident light:

$$d\sigma = \frac{me^2 k \, \omega_{k0} \, V}{2\pi c \hbar^2} \left| Z_{k0} \right|^2 d\Omega ,$$

$$(3.15)$$

where

$$\omega_{k0} = (\gamma + \kappa) \, V_c / \hbar ,$$

$$(3.16)$$

$$d\Omega = (\sin\theta_\kappa) \, d\theta_\kappa \, d\varphi_\kappa ,$$

$$(3.17)$$

$$Z_{k0} = \langle \psi_k(r\theta\varphi) | Z | \psi_0(r\theta\varphi) \rangle .$$

$$(3.18)$$

The detailed expression for (3.18) is given in the Appendix. The dipole approximation, which is assumed in writing (3.15), is expected to be a good approximation when the following conditions are fulfilled:

$$(2.48 \times 10^{-8}) E_0^2 \ll \hbar^2 k^2 / 2m (\text{eV}) \ll 10^6 ,$$

$$(3.19)$$

$$\hbar^2 k^2 / 2m (\text{eV}) \ll 1.24 \times 10^4 / a ,$$

where E_0 is the binding energy of the ground state, (3.2), in units of electron volts, a is the radius of the potential in units of angstrom, and $\hbar^2 k^2 / 2m$ is the energy of the ejected electron. These inequalities correspond to the condition that the wavelength of the incident light must be much larger than the magnitude of the reciprocal wave vector of the ejected electron and also the reciprocal of the potential radius, respectively. Since the binding energies and the transition energies for the systems of our interest fall in the range of a few electron volts, the dipole approximation is valid except at the threshold energy for ionization.

The total cross section σ, which can be obtained by integrating (3.15) over the solid angle, is related to the oscillator strength distribution f by

$$f = (mc/2\pi^2 e^2 \hbar) \sigma .$$

$$(3.20)$$

The cross section was calculated as a function of the transition energy using UNIVAC 418 and the results were drawn by a CALCOMP 565 plotter.

The sum of the oscillator strengths for the ground state should be equal to unity for one-electron problems such as ours (the sum rule). This fact was used to check our computation. We have also found that our photodetachment spectra become identical with Wang's calculations when the magnitude of the parameter λ is increased beyond the region of our interest. When the potential be-

comes deeper so that $\lambda > 4$, the potential accommodates an additional bound state of p type. For such deep potentials, the photodetachment spectra are quite different from those corresponding to $\lambda < 4$ and consist of more than one peak of comparable intensities.
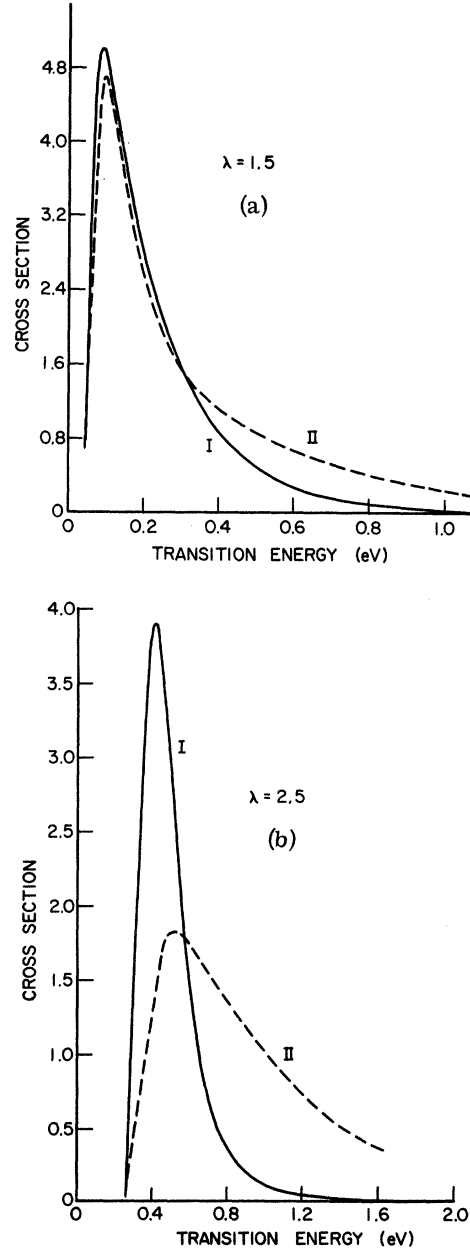
In Fig. 2, we compare the spectra in our calcu-

FIG. 2. Comparison of absorption spectra for the exact continuum wave function (solid line) and the plane-wave approximation (dotted line). (a) and (b) are for $\lambda = 1.5$ and 2.5, respectively. λ is a measure of the binding energy [see Eq. (3.1)]. The radius of the potential is taken to be 5 Å.

lations with those in which the continuum wave functions are approximated by plane waves.[11] It can be seen that the plane-wave model is not a very good approximation for $\lambda > 1.5$, where the effect of the p-wave resonance is significant both in the shape and the peak energy of the spectrum. For the range of the parameters in which the potential has only one bound state, the absorption spectra become more asymmetric for shallow traps: sharp rise near the low-energy threshold and gradual "decay" in the higher-energy side of the peak, while the spectra for deeper traps are less asymmetric because of the interference effect of the p-wave resonance.[12]

IV. MOLECULAR MODEL

The purpose of this section is to present a molecular model for the phenomenological potential of Sec. III. It is convenient to consider the trapping process in two stages of the time scale—before and after the dielectric relaxation. The electron can be localized by inelastic scatterings in the pre-existing fluctuation potential first and then the dielectric relaxation effect sets in to increase the depth of the potential. It is indeed possible to observe the spectrum of an unrelaxed electron either by slowing the relaxation effect at low temperatures[13] or by studying the time dependence of the spectrum.[14] Whether the center of the localization is an intermolecular site (cavity of a certain dimension) or a molecule itself should be decided by calculation rather than choosing arbitrarily. In the following, we consider a theoretical model for the localized states which describes the stage before the dielectric relaxation.

It has been known that the electronic states in disordered structures[15] could contain localized states in addition to extended states, provided fluctuation of potentials exceeds a certain critical value at some locales. An actual quantitative proof of this statement for a given system is not a simple matter, but we assume this to be valid for all the systems in which the absorption spectra have been observed. In order to find the nature of these fluctuating potentials, we start by writing a one-electron Hamiltonian for the excess electron in a given disordered system α as

$$H_\alpha = -\tfrac{1}{2}\Delta + \sum_n v_n(\vec{r} - \vec{R}_n) , \qquad (4.1)$$

where v_n is the electron potential (or pseudopotential) arising from the nth molecule and $\vec{R}_n$ is the coordinate of its center of gravity. Note that v_n is not spherically symmetric in general. The subscript α designates a specific arrangement of molecules, $\alpha(R_1, R_2, \ldots, R_N)$. The eigenfunctions of (4.1) are defined by

$$H_\alpha | \xi_\alpha \rangle = \epsilon_\xi^\alpha | \xi_\alpha \rangle , \qquad \xi = 0, 1, 2, \ldots \qquad (4.2)$$

where ϵ_ξ^α is the ξth eigenvalue and at least the lowest state, $|0_\alpha\rangle$, is assumed to be a localized state.

The transition-moment density corresponding to the transition energy E, $|M(E)|^2$, for an ensemble of disordered structures can be written as

$$| M(E) |^2 = \frac{1}{\Omega \Delta E} \sum_\alpha^{\Delta E} |\langle 0_\alpha | e\vec{r} | \xi_\alpha(E) \rangle|^2 , \qquad (4.3)$$

where the summation is over α and also all the states between E and $E + \Delta E$ for a given structure, and Ω is the number of structures. The transition energy is measured from the ground state for each structure.

One method of calculating (4.3) is to expand $|\xi_\alpha\rangle$ in terms of the Wannier function $|n\rangle$ which is associated with site n:

$$| \xi_\alpha \rangle = \sum_n C_{\xi n}^\alpha | n \rangle , \qquad (4.4)$$

where the coefficients $C_{\xi n}^\alpha$ are to be determined by the variational procedure. Writing the dipole operator $e\vec{r}$ in (4.3) as

$$e\vec{r} = e \sum_n | n \rangle \vec{R}_n \langle n | , \qquad (4.5)$$

we obtain

$$\langle 0_\alpha | e\vec{r} | \xi_\alpha \rangle = e \sum_n \vec{R}_n C_{0n}^\alpha C_{\xi n}^\alpha . \qquad (4.6)$$

Using (4.3) and (4.6), the absorption spectra were computed for a linear chain of 22 nonspherical molecules in our previous work.[16]

The expansion (4.4) in terms of the single-band Wannier functions $|n\rangle$ is equivalent to the approximation of using the projected Hamiltonian of (4.1):

$$PH_\alpha P = \sum_n |n\rangle\langle n| \left[-\tfrac{1}{2}\Delta + \sum_n v_n(\vec{r} - \vec{R}_n) \right] \sum_m |m\rangle\langle m|$$

$$\equiv \sum_n |n\rangle \alpha_{nn} \langle n| + \sum_{n \neq m} |n\rangle \beta_{nm} \langle m| , \qquad (4.7)$$

where α_{nn} is the polarization energy of the electron at site n and β_{nm} is the transfer (or exchange) energy between sites nm. The Wannier functions $|n\rangle$ in practice must be approximated by wave functions either of the negative ion or a low-energy resonance state[12] associated with site n.

If the polarization energy α_{nn} is taken to be a constant, the fluctuation potentials that localize the electron arise from fluctuations in β_{nm}, which is a function of the distance between nm and of their relative orientations.

The physical picture of the trap itself in this model is then a cluster of molecules which happen to have the right configuration in lowering the local electronic energy below the quasifree state.[17] This is essentially a resonance stabilization effect. The simplest such cluster would be a dimer. Since a localized state in three-dimensional space requires exponential decay of the wave function in all directions, the minimum size of the cluster could be greater than 2.

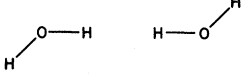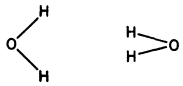When the dielectric relaxation or the local de-

FIG. 3. Relative energies for two water molecules plus an excess electron. The O—O distance is 2.7 Å for all configurations and each molecule has the equilibrium configuration in gas phase (no bond stretching).

formation such as bond stretching takes place, the cluster size is likely to be reduced. It is possible that the center of localization may correspond to a void or cavity in the medium under certain conditions. Some results of our dimer calculations are given in Fig. 3, where each relative energy represents a result of a 21-electron self-consistent-field (SCF) calculation. The absolute energies were found to be sensitive to the choice of wave function for the excess electron. A more detailed description of these calculations will be published separately. [18]

It is important, however, to realize that a detailed calculation, such as Fig. 3, is meaningful in understanding the trapped state itself or the electron spin resonance (ESR) spectrum, but insufficient for the purpose of understanding the optical spectrum. For the latter, equally elaborate calculations for all the excited and ionized states are required. Experimentally observable spectra are the ensemble averages of these molecular calculations.

V. DISCUSSION

The most important factor that we have omitted in our phenomenological model may be the effective mass[9] of the polaron. Electrons in the quasifree state in polar media, or even in nonpolar media, do not necessarily have the same mass as a free electron. The problem requires a much more detailed understanding of the dynamic behavior of the mobile electrons. The relative importance of the long- and short-range potential can also be related

to the magnitude of the effective mass. The problem is further complicated by the possibility of energy dependence of the effective mass and, also, the effect of low-energy resonances arising from fluctuation potentials of disordered structures.

The relevance of our two-parameter potential to real systems is therefore not too clear at this time. By the same token, the meanings of a smooth long-range potential and its $1s \rightarrow 2p$ transition must be studied carefully before one embarks on a detailed calculation or parametrization.

Keeping these uncertainties in mind, and also allowing the possibility of other factors, we have made a comparison of our theoretical results with some experimental results. In these curve-fitting processes, we have not introduced any additional parameters other than the depth and range of the potential. We do not expect a good fit in cases where fluctuation of these two parameters is expected to be important: for example, in low-temperature glasses, or where mixing of other entities such as free radicals is suspected.

In Figs. 4–6, the observed spectra in metal-ammonia solutions, [19] water, [20] and ethanol[13,21] are compared with the results of the two-parameter model. The parameters are summarized in Table I. In these figures, the observed and calculated
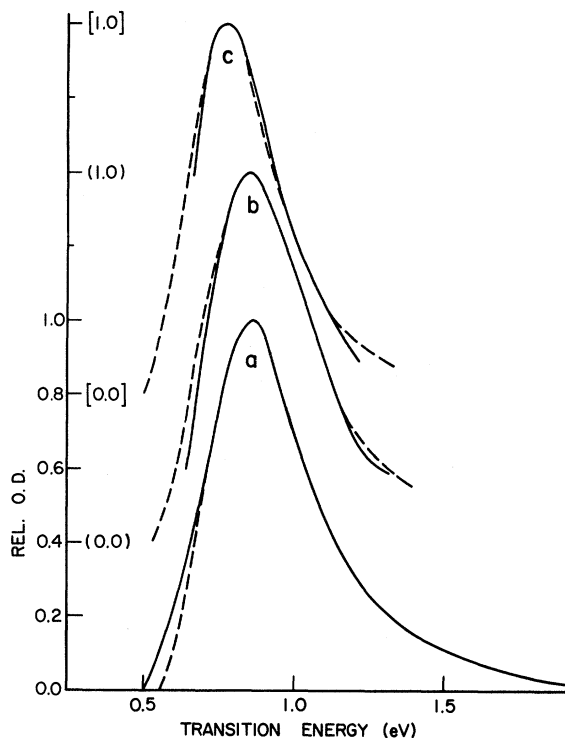

FIG. 4. Comparison of experimental (solid) and theoretical (dotted) absorption spectra for metal-ammonia solutions. The specification of each curve is given in Table I.
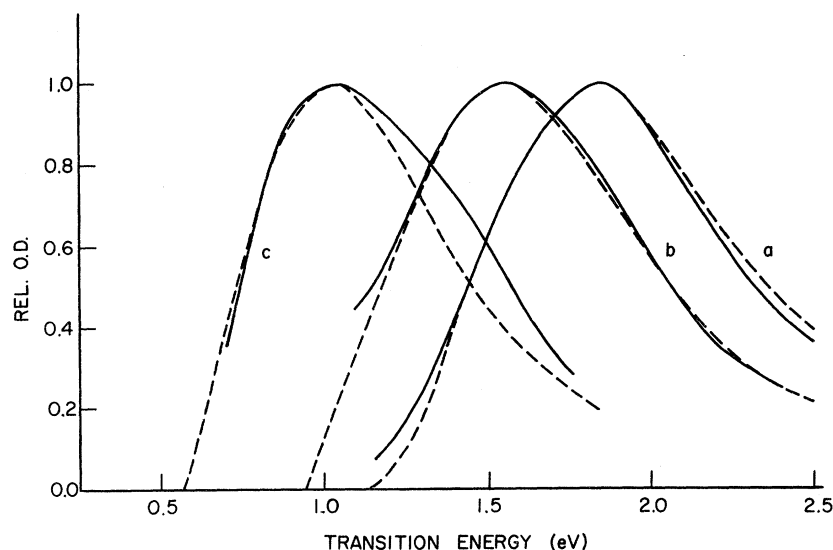
FIG. 5. Comparison of experimental (solid) and theoretical (dotted) absorption spectra for water. The specification of each curve is given in Table I.

spectra are normalized at their peak energies. Coincidence of the transition energies at the peaks therefore has no meaning. Since the theoretical transition energy at the absorption maximum is related to the depth V_0 and the radius a of the potential, the curve-fitting procedure automatically determines the magnitudes of the binding energy E_0 and a, which in turn can be compared with nonoptical experiments. It is clear that experimentally observable quantities, such as the heat of solution and the activation energy for detrapping the electron, are related to the binding energy E_0 [Eq. (3. 2)] rather than the depth of the potential itself. Furthermore, the binding energies relevant for the optical ionization are greater than those for thermal ionization by some unknown factor, probably of the order of 2–3, because of the Franck-Condon principle. It must be remembered, however, that the optimum sets of E_0 and a, which can be obtained from curve fitting, are meaningful only for the square well potentials, which may not be the best model for real potentials.

The experimental information pertinent to E_0 and a is not too abundant. The magnitudes of the radii for metal-ammonia solutions and water in Table

I are consistent with the "cavity" radius,[22] ~ 3.2 Å for the former and the ESR hyperfine structure[23] in ice for the latter.

Comparison with the heat of solution, which was calculated by Copeland, Kestner, and Jortner,[1] is beyond the scope of this paper, because the heat of solution involves the relative energy of the quasifree polaron state with respect to vacuum in addition to the binding energy E_0.

The most striking feature in Figs. 4–6 is the general agreement of the shapes of the spectra, except for the low-temperature glass, ethanol, and water at 300 °C. In water, the spectral profile remains remarkably constant[20] over the temperature range $-4-90$ °C. It is not easy to understand this phenomenon in terms of any simple model. In particular, if the broadness of the spectrum arises

TABLE I. List of parameters.

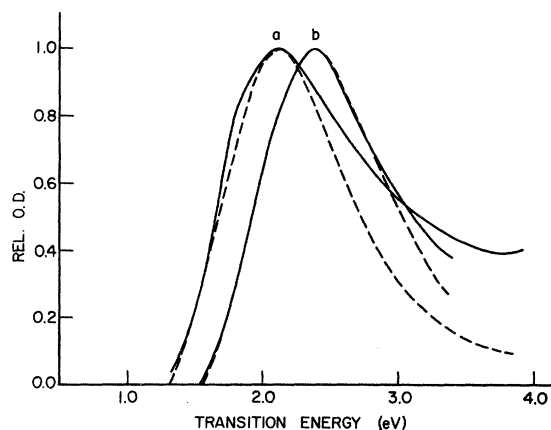| System	Fig.	λ	a (Å)	Temp.	Ref.
Na – NH$_3$, K – NH$_3$	4(a)	2.65	3.63	– 65 °C	12(a)
Na–NH$_3$	4(b)	2.6	3.61	– 70 °C	12(b)
K–NH$_3$	4(c)	2.7	3.88	– 47 °C	12(c)
H$_2$O	5(a)	2.6	2.47	– 4 °C	13
H$_2$O	5(b)	2.5	2.62	90 °C	13
D$_2$O	5(c)	2.3	3.02	300 °C	13
Ethanol	6(a)	2.6	2.30	– 78 °C	14
Ethanol	6(b)	2.65	2.19	77 °K	6

FIG. 6. Comparison of experimental (solid) and theoretical (dotted) absorption spectra for ethanol. The specification of each curve is given in Table I.

from vibronic couplings of $1s \rightarrow 2p$ transition, one would expect an increase of the half-intensity width with temperature. The vibronic coupling alone is not likely to explain the magnitude of the width, which is ~ 0.9 eV in water. This observation may also apply to the case of metal-ammonia solutions.[1]

A recent work by Kawabata[24] indicates the photo-bleaching efficiency of the absorption spectrum of the solvated electron in ice is small for a photon energy lower than that of the absorption maximum. A similar effect has been known in alkanes.[25] This effect has been interpreted to be the manifestation of final states being the bound states, at least in the long-wavelength side of the spectrum. This interpretation is by no means unique. The same effect can be interpreted in the photodetachment scheme such as ours in the following way. The photo-bleaching efficiency is the net result of detrapping and retrapping of electrons. If the retrapping cross section decreases with the energy of the ejected electron, the observed effect can be understood. The most important mechanism for retrapping is likely to be through the low-energy virtual states, which have the property of localized states embedded in the continuum of states. Unless one considers retrapping at the original trap, from which the electron is ejected, these virtual states arise from relatively shallow fluctuation potentials. In this case, only s-wave virtual states are important. The s-wave resonance scattering cross section, as any other resonance cross section, is significant only in a low-energy region[12] and does not vanish at zero energy, unlike the p-wave resonance.

The total oscillator strengths are always unity in our model, while the experimental values for metal-ammonia solutions and water are less than unity. We have no explanation for this discrepancy. It is possible that *ab initio* calculation of the oscillator strength may be beyond the scope of any one-electron scheme.

We have also examined experimental spectra other than those given in Figs. 4–6. The results are similar to those of Figs. 4–6. A relatively large discrepancy was also observed in methanol, as in ethanol of Fig. 6, for the short-wavelength side of the absorption maximum. This discrepancy can be interpreted to arise from absorption of some free radical[26] produced by radiolysis.

Our two-parameter model seems to generate the width and the asymmetry of the absorption spectra with fair accuracy, considering the simplicity of the model. This fact alone does not justify the model itself, but seems to indicate that the model is not totally irrelevant to real systems. Before we proceed to improve the curve fitting, it is imperative to understand at least the qualitative significance of additional parameters. The main problems are the role of high Rydberg states and a more accurate description of the quasifree states in disordered systems.

APPENDIX

The z component of the matrix element, $z_{0\vec{k}}$, in (3.15) can be separated into two factors:

$$z_{0\vec{k}} = z_{0\vec{k},\text{in}} + z_{0\vec{k},\text{out}} , \tag{A1}$$

where

$$z_{0\vec{k},\text{in}} = \langle \psi_k(r\theta\varphi) | z | \psi_0(r\theta\varphi) \rangle_{r<a}$$

$$= V^{-1/2} a^3 A_0 B_{10} (\tfrac{1}{3}\pi^{1/2}) \cos\theta_k \frac{1}{\alpha_c a} \Bigg[\frac{1}{\alpha_c a} \left(\frac{\sin(\alpha_c a - \alpha_0 a)}{\alpha_c a - \alpha_0 a} - \frac{\sin(\alpha_c a + \alpha_0 a)}{\alpha_c a + \alpha_0 a} \right)$$

$$- \left(\frac{\cos(\alpha_c a - \alpha_0 a)}{\alpha_c a - \alpha_0 a} - \frac{\cos(\alpha_c a + \alpha_0 a)}{\alpha_c a + \alpha_0 c} \right) + \left(\frac{\sin(\alpha_c a - \alpha_0 a)}{(\alpha_c a - \alpha_0 a)^2} - \frac{\sin(\alpha_c a + \alpha_0 a)}{(\alpha_c a + \alpha_0 a)^2} \right) \Bigg] , \tag{A2}$$

$$z_{0\vec{k},\text{out}} = \langle \psi_k(r\theta\varphi) | z | \psi_0(r\theta\varphi) \rangle_{r>a}$$

$$= V^{-1/2} a^3 C_0 A'_{10} [\tfrac{1}{3}(4\pi)^{1/2}] \cos\theta_k \frac{e^{-\beta_0 a}}{ka[(ka)^2 + (\beta_0 a)^2]}$$

$$\times \Bigg[\cos\delta_1 \left(\frac{1}{ka}(\beta_0 a \sin ka + ka \cos ka) - (\beta_0 a \cos ka - ka \sin ka) - \frac{1}{(ka)^2 + (\beta_0 a)^2}[(\beta_0^2 a^2 - k^2 a^2)\cos ka - 2ka\beta_0 a \sin ka] \right)$$

$$- \sin\delta_1 \left(-\frac{1}{ka}(\beta_0 a \cos ka - ka \sin ka) - (\beta_0 a \sin ka + ka \cos ka) - \frac{1}{(ka)^2 + (\beta_0 a)^2}[(\beta_0^2 a^2 - k^2 a^2)\sin ka + 2ka\beta_0 a \cos ka] \right)^2 \Bigg] , \tag{A3}$$

$$A'_{10} = 3ie^{-i\delta_1} , \tag{A4}$$

$$B'_{10} = A'_{10} \frac{\cos\delta_1 j_1(ka) - \sin\delta_1 n_1(ka)}{j_1(\alpha_c a)} , \tag{A5}$$

$$A_0 = a^{-1/2}\left(\frac{1}{2} - \frac{\sin 2\alpha_0 a}{4\alpha_0 a} + \frac{\sin^2 \alpha_0 a}{2\beta_0 a}\right)^{-1/2} , \tag{A6}$$

$$C_0 = a^{-1/2} e^{\beta_0 a} \sin\alpha_0 a \left(\frac{1}{2} - \frac{\sin 2\alpha_0 a}{4\alpha_0 a} + \frac{\sin^2 \alpha_0 a}{2\beta_0 a}\right)^{-1/2} , \tag{A7}$$

$$\alpha_0 = (\pi/2a)(\lambda - \gamma)^{1/2} , \tag{A8}$$

$$\beta_0 = (\pi/2a)\gamma^{1/2} . \tag{A9}$$

By inserting (A1)–(A9) into (3.15), it can be easily shown that (3.15) does not depend on V. This can be more clearly expressed as

$$d\sigma = \frac{me^2 k \,\omega_{k0}}{2\pi c\hbar^2} \left| z_{0\vec{k}} \right|^2_{V=1} d\Omega \tag{A10}$$

in the limit of $V \to \infty$.

It should be also mentioned that σ and ω_{k0} depend on a as

$$\sigma \propto a^2 , \tag{A11}$$

$$\omega_{k0} \propto a^{-2} , \tag{A12}$$

when λ and k are fixed. Thus, we can get σ–vs–transition-energy curves at various a very easily from the results calculated at an arbitrarily chosen value of a. The fact that the shape of a σ–vs–transition-energy curve is determined only by λ is very important in our case; otherwise it may be almost impossible to perform the curve-fitting procedure.

[1]D. A. Copeland, N. R. Kestner, and J. Jortner, J. Chem. Phys. 53, 1189 (1970).

[2]G. Breit and E. V. Condon, Phys. Rev. 49, 904 (1936).

[3]B. Duvall and V. Celli, Phys. Letters 26A, 524 (1968).

[4]W. B. Fowler and D. L. Dexter, Phys. Rev. 176, 337 (1968).

[5]T. Miyakawa and D. L. Dexter, Phys. Rev. A 1, 513 (1970).

[6]S. Y. Wang, thesis (University of Michigan, 1967) (unpublished).

[7]See, for example, L. I. Schiff, Quantum Mechanics (McGraw-Hill, New York, 1949).

[8]B. E. Springett, Phys. Letters 35A, 73 (1971).

[9]See, for example, Polarons and Excitons, edited by C. G. Kuper and G. D. Whitfield (Plenum, New York, 1962).

[10]This wave function has the following asymptotic form at large r:

$$\psi_k(r\theta\varphi) \to V^{-1/2}[e^{i\vec{k}\cdot\vec{r}} + r^{-1}f_{\vec{k}}(\theta\varphi) e^{-ikr}] \quad \text{as } r \to \infty .$$

G. Breit and H. A. Bethe, Phys. Rev. 93, 888 (1954).

[11]Ta-You Wu and T. Ohmura, Quantum Theory of Scattering (Prentice-Hall, Englewood Cliffs, N. J., 1962), p. 84.

[12]E. Merzbacher, Quantum Mechanics (Wiley, New York, 1961), p. 237.

[13]H. Hase, M. Noda, and T. Higashimura, J. Chem. Phys. 54, 2975 (1971).

[14]J. H. Baxendale and P. Wardman, Nature 230, 449 (1971).

[15]See, for example, P. W. Anderson, Phys. Rev. 109, 1492 (1958).

[16]K. Funabashi and Y. Maruyama, J. Chem. Phys. 55, 4494 (1971).

[17]B. E. Springett, J. Jortner, and M. H. Cohen, J. Chem. Phys. 48, 2720 (1967).

[18]C. Naleway (unpublished).

[19](a) R. C. Douthit and J. L. Dye, J. Am. Chem. Soc. 82, 4472 (1960); (b) R. K. Quinn and J. J. Lagowski, J. Phys. Chem. 73, 2326 (1969); (c) W. H. Koehler and J. J. Lagowski, ibid. 73, 2329 (1969).

[20]B. D. Michael, E. J. Hart, and K. H. Schmidt, J. Phys. Chem. 75, 2798 (1971).

[21]S. Arai and M. C. Sauer, Jr., J. Chem. Phys. 44, 2297 (1966).

[22]J. Jortner, J. Chem. Phys. 27, 823 (1957).

[23]J. E. Bennett, B. Mile, and A. Thomas, J. Chem. Soc. A, 1393 (1967).

[24]K. Kawabata, J. Chem. Phys. 55, 3672 (1971).

[25]D. W. Skelly and W. H. Hamill, J. Chem. Phys. 43, 2795 (1965).

[26]F. S. Dainton, G. A. Salmon, and J. Teplý, Proc. Roy. Soc. (London) A386, 27 (1965).